Biomechanical Basis of Shoulder Osseous Deformity and Contracture in a Rat Model of Brachial Plexus Birth Palsy

Dustin L. Crouch, PhD, Ian D. Hutchinson, MD, Johannes F. Plate, MD, PhD, Jennifer Antoniono, Hao Gong, MS, Guohua Cao, PhD, Zhongyu Li, MD, PhD, and Katherine R. Saul, PhD

Investigation performed at the Department of Orthopaedic Surgery and Rehabilitation, Wake Forest School of Medicine, Winston-Salem, North Carolina

Background: The purpose of this study was to investigate the relative contributions of two proposed mechanisms, strength imbalance and impaired longitudinal muscle growth, to osseous and postural deformity in a rat model of brachial plexus birth palsy (BPBP).

Methods: Thirty-two Sprague-Dawley rat pups were divided into four groups on the basis of surgical interventions to induce a strength imbalance, impaired growth, both a strength imbalance and impaired growth (a combined mechanism), and a sham condition in the left forelimb. Maximum passive external shoulder rotation angle (ER_{max}) was measured bilaterally at four and eight weeks postoperatively. After the rats were killed at eight weeks, the glenohumeral geometry (on microcomputed tomography) and shoulder muscle architecture properties were measured bilaterally.

Results: Bilateral muscle mass and optimal length differences were greatest in the impaired growth and combined mechanism groups, which also exhibited >15° lower ER_{max} ($p < 0.05$; four weeks postoperatively), 14° to 18° more glenoid declination ($p < 0.10$), and 0.76 to 0.94 mm more inferior humeral head translation ($p < 0.10$) on the affected side. Across all four groups, optimal muscle length was significantly correlated with at least one osseous deformity measure for six of fourteen muscle compartments crossing the shoulder on the affected side ($p < 0.05$). In the strength imbalance group, the glenoid was 5° more inclined and the humeral head was translated 7.5% more posteriorly on the affected side ($p < 0.05$).

Conclusions: Impaired longitudinal muscle growth and shoulder deformity were most pronounced in the impaired growth and combined mechanism groups, which underwent neurectomy. Strength imbalance was associated with osseous deformity to a lesser extent.

Clinical Relevance: Treatments to alleviate shoulder deformity should address mechanical effects of both strength imbalance and impaired longitudinal muscle growth, with an emphasis on developing new treatments to promote growth in muscles affected by BPBP.

Peer Review: This article was reviewed by the Editor-in-Chief and one Deputy Editor, and it underwent blinded review by two or more outside experts. The Deputy Editor reviewed each revision of the article, and it underwent a final review by the Editor-in-Chief prior to publication. Final corrections and clarifications occurred during one or more exchanges between the author(s) and copyeditors.

Upper trunk injury involving the C5 and C6 nerve roots is common in children with brachial plexus birth palsy (BPBP)[1]. As many as 33% of children affected by BPBP sustain permanent osseous and postural shoulder deformity[2]. Typically, osseous shoulder deformity presents as humeral head subluxation, glenoid retroversion, and deformation of the

glenoid articulating surface[3-5]. Deformity is characterized by contracture with limited passive range of motion of shoulder abduction and external rotation[2,6,7]. Osseous deformity is strongly correlated with internal rotation contracture[7], so it is likely that postural and osseous deformities share a common mechanical basis[3].

The prevailing hypothesized mechanism of shoulder deformity is strength imbalance between muscles that internally and externally rotate the shoulder. The infraspinatus, supraspinatus, and teres minor muscles, which augment shoulder external rotation on the basis of their moment arms[8,9], are paralyzed following a C5-C6 injury. Consequently, if unimpaired, the subscapularis and pectoralis major muscles would act unopposed, presumably leading to the development of an internal rotation contracture[10-14]. A second, recently proposed mechanism suggests that impaired longitudinal growth of paralyzed muscles increases the passive force acting on the shoulder. Fibers from the subscapularis muscle, which primarily contributes to internal rotation of the shoulder[8,9], were found to be mechanically stiffer and functionally shorter in infants with BPBP[15]. Additionally, in a mouse model of BPBP, the subscapularis muscle in the affected forelimbs was significantly shorter, smaller, and more fibrotic than the muscle in the unimpaired forelimbs[16].

Evidence supporting the role of either deformity mechanism in the development of shoulder deformity is not consistent across studies. For instance, higher ratios of pectoralis major to external rotator muscle cross-sectional area, indicative of strength imbalance, were associated with increased severity of the glenohumeral deformity[10]. However, excision of the infraspinatus and teres minor in a mouse model of BPBP did not produce internal rotation contractures[16]. Despite evidence of impaired subscapularis and biceps growth and their association with contracture[15-17], the prevalence of external rotation contracture is relatively low[7], even though external rotator muscles (i.e., the supraspinatus and infraspinatus) are frequently involved. Establishing a clearer causal relationship between the two mechanisms and shoulder deformity may guide clinical treatment decisions for BPBP.

We conducted a prospective cohort study in a rat model of BPBP[18,19] to determine the extent to which two deformity mechanisms—strength imbalance and impaired longitudinal muscle growth—contribute to shoulder deformity following BPBP. We allowed both deformity mechanisms to contribute to shoulder deformity independently and in concert. The study hypothesis was that muscle changes associated with strength imbalance would be more strongly related to shoulder deformity than those associated with impaired longitudinal muscle growth.

Materials and Methods

All procedures were approved by the Institutional Animal Care and Use Committee. Thirty-two five-day-old Sprague-Dawley rat pups (Harlan Laboratories, Indianapolis, Indiana) were divided into four groups on the basis of surgical interventions designed to permit strength imbalance or impaired longitudinal muscle growth, or both mechanisms, to contribute to shoulder deformity. The number of rats per group was chosen to detect a difference of 4° of glenoid version between groups (within-group standard deviation = 2.1°)

on the basis of previously obtained computed tomography (CT) measurements[18], with a power of 0.80 using analysis of variance (ANOVA). All surgeries were performed in the left forelimb while the animals were anesthetized with inhaled isoflurane. The animals were closely monitored and given butorphanol tartrate to relieve pain when necessary. In the strength imbalance group, the posterior aspect of the shoulder was injected with botulinum neurotoxin A (BOTOX; Allergan, Irvine, California) to inactivate muscles while leaving their nerves intact, on the basis of a previous BPBP model generated using botulinum toxin[20]. Our strength imbalance model differs from a previous one in which external rotator muscles were excised[16]. In the impaired growth group, rats underwent a neurectomy, used previously to induce BPBP[16,19], of the brachial plexus upper trunk by transverse infraclavicular incision through the pectoralis major muscle. To reduce imbalance between internal and external rotator muscles, botulinum neurotoxin A was injected in the anterior aspect of the shoulder. Botulinum toxin injections were administered when the rats were five days old (1 U/kg dose in a 0.1-mL volume) and at four weeks postoperatively (6 U/kg dose in a 0.1-mL volume) to maintain chemodenervation in the target muscles. Both mechanisms were permitted to contribute to deformity in the combined group in which rats underwent an upper trunk neurectomy only, which is most analogous to the clinical condition. The sham group received infraclavicular incisions and saline solution injections to the anterior and posterior aspects of the shoulder.

Range of Motion

At four and eight weeks postoperatively, we measured the maximum passive external shoulder rotation angle (ER_{max}) bilaterally. Time points correspond to approximately 3.1 and 5.8 years of postnatal human musculoskeletal development[21], by which time shoulder deformity is well established clinically. The ER_{max} was measured using a custom test fixture while the animals were under anesthesia with inhaled isoflurane (Fig. 1). The forelimb was placed in 90° of shoulder abduction and 90° of elbow flexion, with the limb oriented ventrally at a neutral shoulder rotation posture[19]. During the examination, electromyographic (EMG) signals were recorded from the pectoralis major muscle using stainless-steel fine wire electrodes inserted percutaneously into the muscle belly. The individual who performed the measurements was not blinded to treatment group.
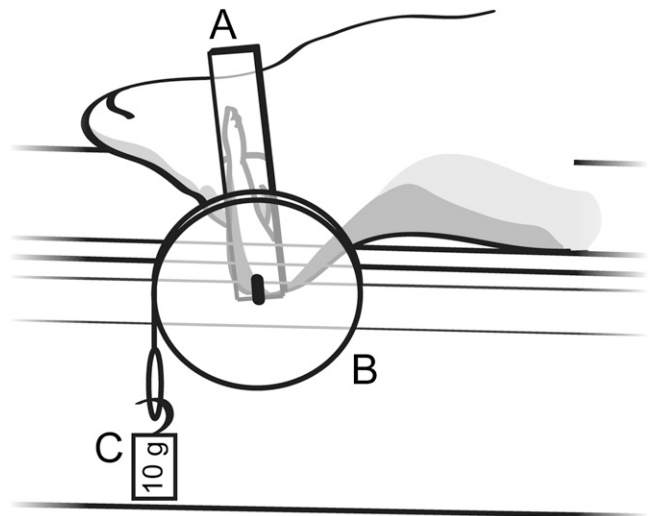

Fig. 1

Custom test fixture used to measure the maximum passive external shoulder rotation angle (ER_{max}). The forearm was fixed against a rotating arm (A) that was connected by an axle to a 1-in (2.54-cm) circular disc (B). A 10-g weight hung from the disc rim (C) applied a constant external rotational force at the shoulder. The ER_{max} was measured using a protractor (not shown).

TABLE I Pearson Correlation Coefficient (r) Between Optimal Muscle Length and Shoulder Deformity Measurements from the Affected Forelimbs						
	Range of Motion at Week 8	Version	Inclination	Anteroposterior Subluxation	Superoinferior Translation	Glenoid Curvature
External rotators						
Supraspinatus	−0.33	0.02	−0.03	−0.10	−0.07	−0.01
Spinodeltoid	0.02	−0.30	0.54*	−0.40*	0.50*	−0.50*
Infraspinatus	−0.28	−0.02	0.11	−0.23	0.03	−0.21
Teres minor	−0.06	−0.14	0.27	−0.22	0.26	−0.31
Deltoid, posterior	−0.06	−0.18	0.36*	−0.40*	0.36*	−0.33
Internal rotators						
Pectoralis, clavicular	−0.23	0.02	0.09	−0.10	0.08	−0.10
Pectoralis, sternal	−0.41*	0.05	0.06	0.05	0.02	−0.07
Teres major	0.31	−0.41*	0.59*	−0.36*	0.58*	−0.62*
Subscapularis, upper	0.09	−0.29	0.36*	−0.30	0.30	−0.40*
Subscapularis, lower	0.33	−0.30	0.55*	−0.27	0.55*	−0.50*
Deltoid, anterior	−0.18	0.00	0.24	−0.25	0.24	−0.24
Biceps, long head	−0.31	0.17	−0.18	0.23	−0.17	0.43*
Biceps, short head	−0.31	−0.14	0.11	−0.30	0.06	−0.16
Triceps, long head	−0.31	−0.22	−0.04	0.10	−0.19	−0.17

*$P < 0.05$.

Specimen Preparation

At eight weeks postoperatively, the animals were killed through intracardiac injection of saturated potassium chloride, consistent with the recommendations of the American Veterinary Medical Association. The torso and forelimbs were skinned and secured to metal plates to position the forelimbs in approximately 20° of shoulder abduction, neutral shoulder flexion and rotation, 90° of elbow flexion, and neutral forearm pronation-supination. The secured specimens were fixed in 10% phosphate-buffered formalin for forty-eight hours and then were immersed in phosphate-buffered saline solution for storage[22].

Microcomputed Tomographic (Micro-CT) Imaging and Analysis

Both forelimb shoulders of the fixed specimens were imaged in a micro-CT scanner (MicroXCT-400; Xradia, Pleasanton, California). For each scan, 805 projections were acquired over an angular range from −96° to 96°. Pixel width was 85 μm. Bones were segmented automatically in Mimics software (Materialise, Leuven, Belgium) using a custom bone threshold (image conversion to Hounsfield units was not performed). Anatomical measurements made from the reconstructed three-dimensional volumetric images included glenoid version, glenoid inclination angle, and superoinferior translation and anteroposterior subluxation of the humeral head relative to the glenoid. Glenoid version and anteroposterior subluxation were measured in a manner similar to clinical techniques[23]. The glenoid inclination angle was measured within the plane of the subscapular fossa by subtracting 90° from the superolateral angle between the scapular spine centerline and a line tangent to the glenoid fossa rim. Superoinferior translation was measured as the smallest distance between the humeral head and a plane aligned to the scapular spine. The individual performing the measurements was not blinded to treatment group.

Muscle Architecture

Ten muscles crossing the glenohumeral joint were dissected bilaterally from the fixed specimens: deltoid, pectoralis major (sternoclavicular head), supraspinatus, infraspinatus, spinodeltoid (not found in humans), subscapularis, teres major, teres minor, biceps brachii, and triceps (long head). Compartments of the biceps brachii (long and short heads), deltoid (anterior and posterior), subscapularis (upper and lower), and pectoralis major (sternal and clavicular heads) were sectioned along connective tissue that delineated the compartment boundaries. Mass, muscle-tendon length, muscle length, and sarcomere length were measured directly for each muscle. Mass was measured on a digital scale with a resolution of 0.1 μg. Before muscle mass was measured, extramuscular tendon and connective tissue were removed and muscles were blotted dry. Muscle-tendon length, muscle length, and sarcomere length were measured using digital calipers with a resolution of 0.01 mm. Sarcomere length was measured with a standard laser diffraction technique[24] using a 5.0-mW HeNe laser with a wavelength of 633 nm (Thorlabs, Newton, New Jersey). The laser diffraction projected light bands, and the spacing between the bands was measured using calipers. Optimal muscle length (L_0^m) was computed by normalizing muscle length by sarcomere length[22]:

$$L_0^m = L^m \left(\frac{2.4 \mu m}{L^s} \right)$$

In the equation, L^m and L^s are muscle length and sarcomere length, respectively. Optimal sarcomere length was assumed to be 2.4 μm for rat skeletal muscle[25]. The individual performing the measurements was blinded to treatment group but not to side (right or left).

Data Analysis

Paired Student t tests were performed to compare ER_{max}, muscle properties, and bone geometry between the affected (left) and unaffected (right) forelimbs for each group. As an estimate of internal-external rotation strength imbalance, we calculated the ratio between internal rotator (pectoralis major and subscapularis) and external rotator (supraspinatus, infraspinatus, and spinodeltoid) muscle mass. The strength ratio was compared among groups using a one-way ANOVA with a post hoc Tukey test to identify between-group differences. Finally, data were combined across groups to determine, using the Pearson correlation coefficient (r), whether optimal muscle length correlated with ER_{max} and anatomical bone geometry measurements from the affected sides. Comparisons were significant at $p < 0.05$.
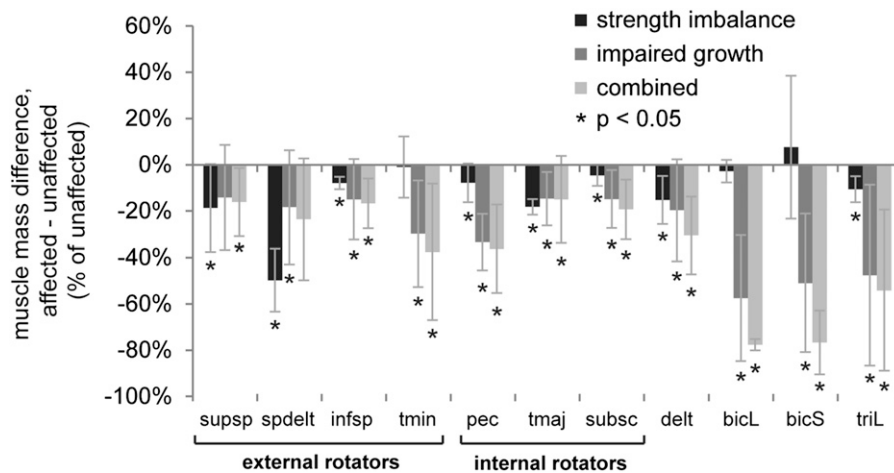
Fig. 2

Muscle mass difference between the affected (left) and unaffected (right) forelimbs. Muscle mass was significantly lower in groups that received an upper trunk neurectomy. Each bar and whisker represent the mean and the standard deviation. Supsp = supraspinatus, spdelt = spinodeltoid, infsp = infraspinatus, tmin = teres minor, pec = pectoralis major, tmaj = teres major, subsc = subscapularis, delt = deltoid, bicL = biceps brachii (long head), bicS = biceps brachii (short head), and triL = triceps brachii (long head).

Results

Muscle Mass

Nine of ten dissected muscles were significantly atrophic on the affected side in the impaired growth and combined groups, which received an upper trunk neurectomy (Fig. 2). In the impaired growth group, biceps and triceps muscle mass was a mean of 55% (p < 0.001) and 48% (p = 0.006) lower, respectively, on the affected side. Likewise, in the combined group, biceps and triceps muscle mass was a mean of 77% (p < 0.001) and 54% (p = 0.002) lower, respectively, on the affected side. In the strength imbalance group, the mass of the supraspinatus, infraspinatus, and spinodeltoid muscles, which externally rotate the shoulder, was 19% (p = 0.008), 8% (p < 0.001), and 50% (p < 0.001) lower, respectively, on the affected side. In the sham group, the pectoralis major had significantly lower muscle mass on the affected side, presumably because of splitting the pectoralis major as part of the neurectomy procedure. The ratio of internal rotator to external rotator muscle mass was significantly higher in the strength imbalance group than in other groups (p < 0.001) (Fig. 3).

Optimal Muscle Length

Bilateral optimal muscle length differences, an indicator of impaired longitudinal muscle growth, were largest in the impaired growth and combined groups, which underwent neurectomy (Fig. 4). In the impaired growth group, the mean optimal muscle length was significantly shorter (p < 0.05) on the affected side for two internal rotator muscles (pectoralis major [12%] and teres major [10%]) and the short head of the biceps [11%]. Similarly, in the combined group, the mean

optimal muscle length was significantly shorter (p < 0.05) on the affected side for three internal rotator muscles (pectoralis major [14%]), subscapularis [13%], and teres major [11%]) and one external rotator muscle (supraspinatus [4%]). In the strength imbalance group, spinodeltoid and teres major optimal muscle lengths were significantly shorter on the affected side.

Postural Deformity

The mean ER_{max} was 26° (p = 0.03) and 23° (p = 0.004) lower in the affected limbs in the impaired growth group at four and eight weeks, respectively, compared with the unaffected side (Fig. 5). Likewise, the mean range of motion was 17° (p = 0.006) and 11°
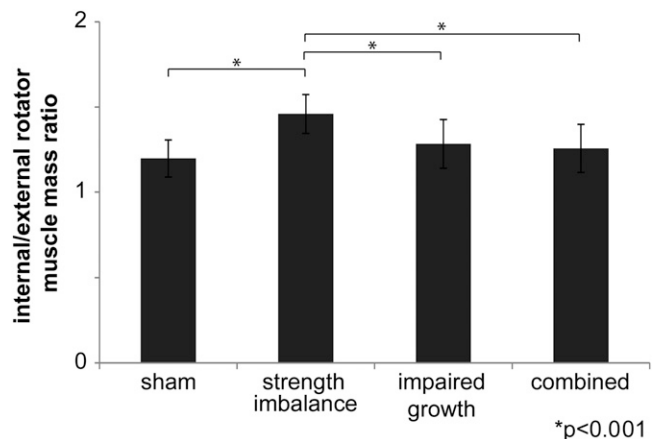

Fig. 3

Ratio of internal rotator (pectoralis major and subscapularis) to external rotator (supraspinatus, infraspinatus, and spinodeltoid) muscle mass. Internal-external rotator muscle mass ratio was significantly higher in the strength imbalance group than in the other three groups. Each bar and whisker represent the mean and the standard deviation.

BIOMECHANICAL BASIS OF SHOULDER OSSEOUS DEFORMITY IN A
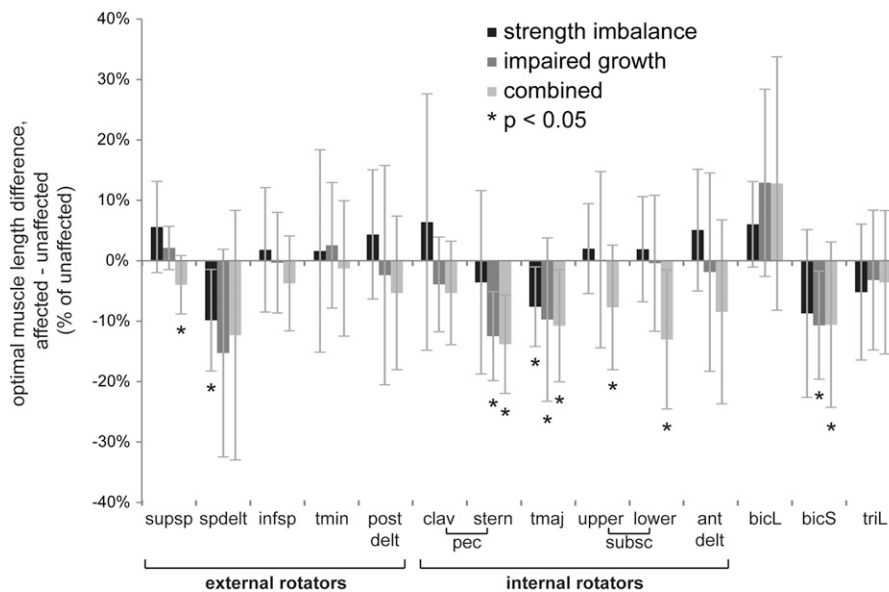RAT MODEL OF BRACHIAL PLEXUS BIRTH PALSY

Fig. 4

Optimal muscle length difference between the affected (left) and unaffected (right) forelimbs. The bilateral difference in optimal muscle length, an indicator of impaired longitudinal muscle growth, was largest in the impaired growth and combined groups. Each bar and whisker represent the mean and the standard deviation. Supsp = supraspinatus, spdelt = spinodeltoid, infsp = infraspinatus, tmin = teres minor, delt = deltoid, clav pec = pectoralis major (clavicular head), stern pec = pectoralis major (sternal head), tmaj = teres major, subsc = subscapularis, bicL = biceps brachii (long head), bicS = biceps brachii (short head), and triL = triceps brachii (long head).

(p = 0.10) lower in the affected limbs in the combined group at four and eight weeks, respectively. The strength imbalance groups had significantly higher ER_{max} at four weeks, possibly because of increased passive external rotation forces with impaired growth of the spinodeltoid. No muscle activity was observed in the EMG recordings during the passive external shoulder rotation trials.

Osseous Deformity

Bilateral glenohumeral geometry differences were most pronounced in the impaired growth and combined groups. The glenoid was more declined in the impaired growth and combined groups on the affected side (mean inclination, −52.3° [p = 0.07] and −56.1° [p = 0.02], respectively) than on the unaffected side (mean inclination, −37.4° and −38.4°, respectively) (Fig. 6). Conversely, in the strength imbalance group, the affected glenoid was less declined than the unaffected glenoid (mean inclination, −33.1° and −38.4°, respectively; p = 0.01). The affected glenoid was 20.7° more anteverted in the impaired growth group (p = 0.11), but 7.7° more retroverted in the combined group (p = 0.10), compared with the unaffected glenoid. In the impaired growth and combined groups, the humeral head was translated more inferiorly on the affected side (mean, 0.86 and 1.03 mm inferior translation, respectively) than on the unaffected side (mean, 0.10 [p = 0.07] and 0.09 mm [p = 0.09] superior translation, respectively) (Fig. 7). In the strength imbalance group, the humeral head was translated more posteriorly on the affected side (mean, 61.5%) than on the unaffected side (mean, 69%; p = 0.04).

Correlation Between Optimal Muscle Length and Shoulder Deformity

Across all groups, optimal muscle length was significantly correlated with at least one shoulder osseous deformity measure on the affected side for the posterior deltoid, spinodeltoid, subscapularis, teres major, and long head of the biceps muscles
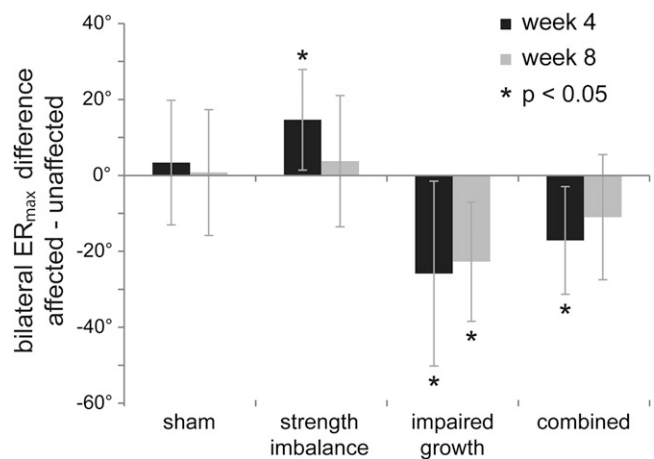

Fig. 5

Bilateral difference in maximum passive external shoulder rotation angle, ER_{max} (affected − unaffected). Negative values indicated lower ER_{max} on the affected side. The ER_{max} was significantly lower in groups that received an upper trunk neurectomy. The ER_{max} was not lower on average in the sham and strength imbalance groups at both four and eight weeks. Each bar and whisker represent the mean and the standard deviation.
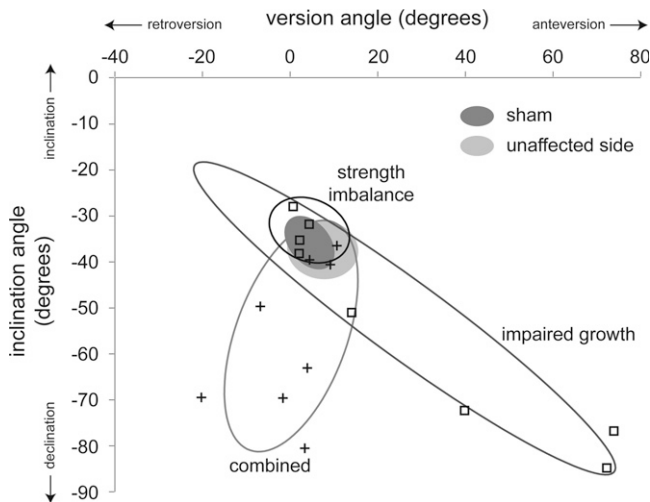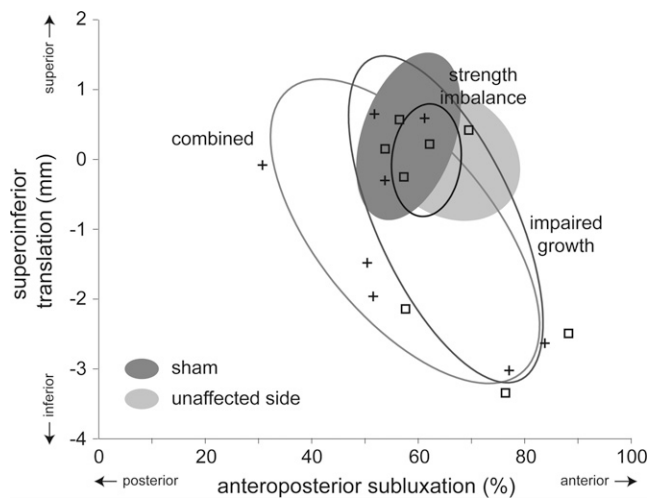
Fig. 6 Glenoid version and inclination angles in affected forelimbs. Ovals represent 68% confidence regions of measures from the affected sides of each group, and from the unaffected side combined across all groups. Individual measurements are shown for the impaired growth (squares) and combined (plus symbols) groups. The glenoid inclination angle was higher on the affected side in the strength imbalance group (p = 0.01), but lower on the affected side in the impaired growth (p = 0.07) and combined (p = 0.02) groups, compared with the unaffected side. Glenoid version and inclination were similar between the sham group and the unaffected sides. **Fig. 7** Anteroposterior subluxation and superoinferior translation of the humeral head relative to the scapula. Ovals represent 68% confidence regions of measures from the affected sides of each group, and from the unaffected side combined across all groups. Individual measurements are shown for the impaired growth (squares) and combined (plus symbols) groups. In both the impaired growth and combined groups, the humeral head was translated more inferiorly on the affected side than on the unaffected side (p = 0.07 and p = 0.09, respectively). Conversely, the humeral head was translated more posteriorly on the affected side in the strength imbalance group (p = 0.04). In the sham group, the affected humeral head was slightly posteriorly subluxated (p = 0.03) compared with the unaffected side.

(Table I). There was a significant negative correlation between pectoralis major optimal length and ER_{max} on the affected side, which was counterintuitive since the pectoralis major internally rotates the shoulder. However, optimal muscle length of other internal rotator muscles, such as the teres major and the subscapularis, was weakly (but not significantly) positively correlated with ER_{max}.

Discussion

Both impaired longitudinal muscle growth and strength imbalance mechanisms are capable of producing shoulder deformity following BPBP[26], but strength imbalance has long been considered the predominant deformity mechanism. In our study, the strength imbalance group exhibited the highest ratio of internal to external rotator muscle mass of all of the experimental groups, but did not develop severe contracture or deformity. In patients, osseous glenohumeral deformity was significantly correlated with internal-external rotator muscle mass ratio[10] and contracture[7]. Our findings corroborate those of a previous muscle excision-induced strength imbalance mouse model[16]. Altered cross-sectional area or antagonist muscle mass ratios only indicate an imbalance of force-generating capacity, and may not appropriately reflect the actual mechanical loading of the glenohumeral joint. Increased muscle activity of dually innervated unimpaired muscles[27] could alter glenohumeral mechanical loading[26], but whether such loads are sufficient to cause deformity remains unknown.

Impaired longitudinal muscle growth, observed clinically[15], has been associated with contracture in previous animal models of BPBP[16,17]. Likewise, groups that underwent neurectomy (the impaired growth and combined groups) also exhibited the most pronounced impaired longitudinal growth of internal rotator muscles and the most severe internal rotation contractures (limited ER_{max} on the affected side). Additionally, low optimal muscle length was significantly correlated with osseous shoulder deformity for external rotator (posterior deltoid and spinodeltoid) and internal rotator (teres major and subscapularis) muscles across all groups. In three-day-old mice, delayed addition of serial sarcomeres (impaired longitudinal growth) in denervated soleus muscle was attributed to reduced muscle excursion as a consequence of denervation[28]. It is also possible that certain conditions, including strength imbalance and severe weakness, may effectively immobilize muscles in a lengthened or shortened position, potentially altering optimal muscle lengths[29]. Since excursion is regarded as an important sarcomere-regulating factor[30], passive stretching by application of a cast or passive manipulation of the upper limb may reduce contracture severity in children with BPBP[31,32]; however, more research is needed to quantify its efficacy.

The strength imbalance group, in which the spinodeltoid and teres major muscles had both significantly lower mass and optimal length on the affected side, included aspects of a combined mechanism model, albeit with higher internal-external rotator imbalance and fewer muscles with impaired growth than observed in the combined group. Although the strength imbalance mechanism was

not purely isolated as we intended, our principal finding remains that more extensive impaired longitudinal muscle growth was associated with more severe shoulder deformity, while more pronounced strength imbalance conditions were not. Additionally, muscle changes presumably induced by chemodenervation, along with absent EMG activity during range-of-motion measurements, provide insight into the variable outcomes achieved when botulinum toxin has been used to relieve contractures in children with BPBP[33].

The combined group exhibited glenoid retroversion similar to clinical cases[3], but the glenoid was anteverted in the impaired growth group. Glenoid anteversion was possibly related to botulinum toxin injections that the group received in the anterior aspect of the shoulder. Additionally, the subscapularis, which applies a posteriorly directed force on the glenoid[26], was significantly shorter in the combined group but not in the impaired growth group, possibly explaining why glenoid retroversion was observed only in the combined group.

To our knowledge, inferior humeral head translation, observed in the impaired growth and combined groups, has not been previously investigated in clinical cases. Observations of inferior translation corresponded with impaired growth of muscles that depress the humerus on the basis of their lines of action at the glenohumeral joint, including the pectoralis major (impaired growth and combined groups) and subscapularis (combined group only). Similarly, significant posterior humeral head translation in the strength imbalance group was possibly due to impaired growth of the spinodeltoid and the teres major, which apply a posteriorly directed force on the humerus on the basis of their lines of action.

We observed global patterns of muscle atrophy, although we expect that interventions were more localized. Similarly, children with incomplete BPBP may present with globally impaired growth of the affected upper limb[34]. Weakness or paralysis of muscles directly impaired by the interventions could contribute to limb disuse and global atrophy. It is also possible that injury induced by neurectomy and chemodenervation was more widespread than intended, given the challenges of operating on rat pups.

There were several limitations of our study. Although shoulder neuromusculoskeletal anatomy between rats and humans is similar[35], glenohumeral mechanical loading differs between the species since rats are lifelong quadrupeds, while infants may crawl only within their first year. In the sham group, muscle changes were induced by splitting the pectoralis major, but these changes did not appear to contribute substantially to shoulder deformity in the sham group, while deformity was more pronounced in the groups that underwent neurectomy. It was difficult to clearly define the musculotendinous junctions of some muscles, notably the biceps, which may have contributed to measurement error of in situ muscle lengths used to compute optimal muscle lengths. High within-group variability in the study outcomes may

be due to variable spontaneous neuromuscular recovery[36] or surgery effects. Since the investigators were not blinded to treatment group when measuring ER_{max} and bone geometry, these values may have been influenced by detection bias.

In summary, impaired longitudinal muscle growth was more strongly associated with severe shoulder deformity than were strength imbalance conditions in rats that underwent neurectomy. Clinical management of BPBP must address the clear and substantial role that impaired longitudinal muscle growth appears to play in the development of shoulder deformity. ∎

Dustin L. Crouch, PhD
UNC-NCSU Joint Department of Biomedical Engineering,
North Carolina State University,
911 Oval Drive,
Engineering Building 3,
Campus Box 7115,
Raleigh, NC 27695.
E-mail address: dlcrouch@ncsu.edu

Ian D. Hutchinson, MD
Johannes F. Plate, MD, PhD
Zhongyu Li, MD, PhD
Department of Orthopaedic Surgery and Rehabilitation,
Wake Forest School of Medicine,
Medical Center Boulevard,
Winston-Salem, NC 27103.
E-mail address for I.D. Hutchinson: ihutchin@wakehealth.edu.
E-mail address for J.F. Plate: jplate@wakehealth.edu.
E-mail address for Z. Li: zli@wakehealth.edu

Jennifer Antoniono
Katherine R. Saul, PhD
Department of Mechanical and Aerospace Engineering,
North Carolina State University,
911 Oval Drive,
Engineering Building 3,
Campus Box 7910,
Raleigh, NC 27695.
E-mail address for J. Antoniono: jmantoni@ncsu.edu.
E-mail address for K.R. Saul: ksaul@ncsu.edu

Hao Gong, MS
Guohua Cao, PhD
Virginia Tech-Wake Forest School of Biomedical
Engineering and Sciences,
Virginia Polytechnic Institute and State University,
Kelly Hall, 325 Stanger Street,
MC 0298, Blacksburg, VA 24061.
E-mail address for H. Gong: haog1@vt.edu.
E-mail address for G. Cao: ghcao@vt.edu

References

1. Lagerkvist AL, Johansson U, Johansson A, Bager B, Uvebrant P. Obstetric brachial plexus palsy: a prospective, population-based study of incidence, recovery, and residual impairment at 18 months of age. Dev Med Child Neurol. 2010 Jun;52 (6):529-34. Epub 2009 Dec 23.

2. Pearl ML. Shoulder problems in children with brachial plexus birth palsy: evaluation and management. J Am Acad Orthop Surg. 2009 Apr;17(4):242-54.

3. Pearl ML, Edgerton BW. Glenoid deformity secondary to brachial plexus birth palsy. J Bone Joint Surg Am. 1998 May;80(5):659-67.

BIOMECHANICAL BASIS OF SHOULDER OSSEOUS DEFORMITY IN A
RAT MODEL OF BRACHIAL PLEXUS BIRTH PALSY

4. Hogendoorn S, van Overvest KLJ, Watt I, Duijsens AHB, Nelissen RGHH. Structural changes in muscle and glenohumeral joint deformity in neonatal brachial plexus palsy. J Bone Joint Surg Am. 2010 Apr;92(4):935-42.

5. Pöyhiä TH, Nietosvaara YA, Remes VM, Kirjavainen MO, Peltonen JI, Lamminen AE. MRI of rotator cuff muscle atrophy in relation to glenohumeral joint incongruence in brachial plexus birth injury. Pediatr Radiol. 2005 Apr;35(4):402-9. Epub 2005 Jan 6.

6. Nath RK, Mahmooduddin F, Liu X, Wentz MJ, Humphries AD. Coracoid abnormalities and their relationship with glenohumeral deformities in children with obstetric brachial plexus injury. BMC Musculoskelet Disord. 2010;11:237. Epub 2010 Oct 13.

7. Hoeksma AF, Ter Steeg AM, Dijkstra P, Nelissen RG, Beelen A, de Jong BA. Shoulder contracture and osseous deformity in obstetrical brachial plexus injuries. J Bone Joint Surg Am. 2003 Feb;85(2):316-22.

8. Otis JC, Jiang CC, Wickiewicz TL, Peterson MG, Warren RF, Santner TJ. Changes in the moment arms of the rotator cuff and deltoid muscles with abduction and rotation. J Bone Joint Surg Am. 1994 May;76(5):667-76.

9. Kuechle DK, Newman SR, Itoi E, Niebur GL, Morrey BF, An KN. The relevance of the moment arm of shoulder muscles with respect to axial rotation of the glenohumeral joint in four positions. Clin Biomech (Bristol, Avon). 2000 Jun;15(5):322-9.

10. Waters PM, Monica JT, Earp BE, Zurakowski D, Bae DS. Correlation of radiographic muscle cross-sectional area with glenohumeral deformity in children with brachial plexus birth palsy. J Bone Joint Surg Am. 2009 Oct;91(10):2367-75.

11. Hale HB, Bae DS, Waters PM. Current concepts in the management of brachial plexus birth palsy. J Hand Surg Am. 2010 Feb;35(2):322-31.

12. Birch R, Bonney G, Parry CBW, editors. Surgical disorders of the peripheral nerves. 2nd ed. Edinburgh: Churchill Livingstone; 1998. p 209-33.

13. Dodds SD, Wolfe SW. Perinatal brachial plexus palsy. Curr Opin Pediatr. 2000 Feb;12(1):40-7.

14. van Gelein Vitringa VM, van Kooten EO, Mullender MG, van Doorn-Loogman MH, van der Sluijs JA. An MRI study on the relations between muscle atrophy, shoulder function and glenohumeral deformity in shoulders of children with obstetric brachial plexus injury. J Brachial Plex Peripher Nerve Inj. 2009 May 18;4:5.

15. Einarsson F, Hultgren T, Ljung BO, Runesson E, Fridén J. Subscapularis muscle mechanics in children with obstetric brachial plexus palsy. J Hand Surg Eur Vol. 2008 Aug;33(4):507-12.

16. Nikolaou S, Peterson E, Kim A, Wylie C, Cornwall R. Impaired growth of denervated muscle contributes to contracture formation following neonatal brachial plexus injury. J Bone Joint Surg Am. 2011 Mar 2;93(5):461-70.

17. Weekley H, Nikolaou S, Hu L, Eismann E, Wylie C, Cornwall R. The effects of denervation, reinnervation, and muscle imbalance on functional muscle length and elbow flexion contracture following neonatal brachial plexus injury. J Orthop Res. 2012 Aug;30(8):1335-42. Epub 2012 Jan 6.

18. Li Z, Barnwell J, Tan J, Koman LA, Smith BP. Microcomputed tomography characterization of shoulder osseous deformity after brachial plexus birth palsy: a rat model study. J Bone Joint Surg Am. 2010 Nov 3;92(15):2583-8.

19. Li Z, Ma J, Apel P, Carlson CS, Smith TL, Koman LA. Brachial plexus birth palsy-associated shoulder deformity: a rat model study. J Hand Surg Am. 2008 Mar;33(3):308-12.

20. Kim HM, Galatz LM, Patel N, Das R, Thomopoulos S. Recovery potential after postnatal shoulder paralysis. An animal model of neonatal brachial plexus palsy. J Bone Joint Surg Am. 2009 Apr;91(4):879-91.

21. Quinn R. Comparing rat's to human's age: how old is my rat in people years? Nutrition. 2005 Jun;21(6):775-7.

22. Ward SR, Sarver JJ, Eng CM, Kwan A, Würgler-Hauri CC, Perry SM, Williams GR, Soslowsky LJ, Lieber RL. Plasticity of muscle architecture after supraspinatus tears. J Orthop Sports Phys Ther. 2010 Nov;40(11):729-35.

23. Waters PM, Smith GR, Jaramillo D. Glenohumeral deformity secondary to brachial plexus birth palsy. J Bone Joint Surg Am. 1998 May;80(5):668-77.

24. Lieber RL, Yeh Y, Baskin RJ. Sarcomere length determination using laser diffraction. Effect of beam and fiber diameter. Biophys J. 1984 May;45(5):1007-16.

25. Burkholder TJ, Lieber RL. Sarcomere length operating range of vertebrate muscles during movement. J Exp Biol. 2001 May;204(Pt 9):1529-36.

26. Crouch DL, Plate JF, Li Z, Saul KR. Computational sensitivity analysis to identify muscles that can mechanically contribute to shoulder deformity following brachial plexus birth palsy. J Hand Surg Am. 2014 Feb;39(2):303-11. Epub 2013 Dec 15.

27. Newman CJ, Morrison L, Lynch B, Hynes D. Outcome of subscapularis muscle release for shoulder contracture secondary to brachial plexus palsy at birth. J Pediatr Orthop. 2006 Sep-Oct;26(5):647-51.

28. Williams PE, Goldspink G. The effect of denervation and dystrophy on the adaptation of sarcomere number to the functional length of the muscle in young and adult mice. J Anat. 1976 Nov;122(Pt 2):455-65.

29. Williams PE, Goldspink G. The effect of immobilization on the longitudinal growth of striated muscle fibres. J Anat. 1973 Oct;116(Pt 1):45-55.

30. Koh TJ, Herzog W. Excursion is important in regulating sarcomere number in the growing rabbit tibialis anterior. J Physiol. 1998 Apr 1;508(Pt 1):267-80.

31. De Deyne PG. Application of passive stretch and its implications for muscle fibers. Phys Ther. 2001 Feb;81(2):819-27.

32. Ramos LE, Zell JP. Rehabilitation program for children with brachial plexus and peripheral nerve injury. Semin Pediatr Neurol. 2000 Mar;7(1):52-7.

33. Gobets D, Beckerman H, de Groot V, Van Doorn-Loogman MH, Becher JG. Indications and effects of botulinum toxin A for obstetric brachial plexus injury: a systematic literature review. Dev Med Child Neurol. 2010 Jun;52(6):517-28. Epub 2010 Feb 12.

34. Bae DS, Ferretti M, Waters PM. Upper extremity size differences in brachial plexus birth palsy. Hand (N Y). 2008 Dec;3(4):297-303. Epub 2008 Apr 25.

35. Norlin R, Hoe-Hansen C, Oquist G, Hildebrand C. Shoulder region of the rat: anatomy and fiber composition of some suprascapular nerve branches. Anat Rec. 1994 Jul;239(3):332-42.

36. Brenner MJ, Moradzadeh A, Myckatyn TM, Tung TH, Mendez AB, Hunter DA, Mackinnon SE. Role of timing in assessment of nerve regeneration. Microsurgery. 2008;28(4):265-72.